Environmental Science
Processes & Impacts

RSC Publishing

PAPER

View Article Online
View Journal | View Issue

Open Access Article. Published on 18 October 2013. Downloaded on 9/6/2024 8:07:53 AM.
This article is licensed under a Creative Commons Attribution 3.0 Unported Licence.

Cite this: *Environ. Sci.: Processes Impacts*, 2013, **15**, 2263

Exploring the potential influence of climate change and particulate organic carbon scenarios on the fate of neutral organic contaminants in the Arctic environment†

James M. Armitage*[ab] and Frank Wania[a]

Received 18th June 2013
Accepted 8th October 2013

DOI: 10.1039/c3em00315a

rsc.li/process-impacts

The main objective of this study is to explore the potential influence of climate change and particulate organic carbon scenarios on the fate of organic chemicals in the Arctic marine environment using an evaluative modeling approach. Particulate organic carbon scenarios are included to represent changes such as enhanced primary production and terrestrial inputs. Simulations are conducted for a set of hypothetical chemicals covering a wide range of partitioning property combinations using a 40-year emission scenario. Differences in model output between the default simulations (*i.e.* contemporary conditions) and future scenarios during the primary emission phase are limited in magnitude (typically within a factor of two), consistent with other modeling studies. The changes to particulate organic carbon levels in the Arctic Ocean assumed in the simulations exert a relatively important influence for hydrophobic organic chemicals during the primary emission phase, mitigating the potential for exposure *via* the pelagic food web by reducing freely-dissolved concentrations in the water column. The changes to particulate organic carbon levels are also influential in the secondary emission/depuration phase. The model results illustrate the potential importance of changes to organic carbon levels in the Arctic Ocean and support efforts to improve the understanding of organic carbon cycling and links to climate change.

Environmental impact

This study presents the results of an evaluative modelling exercise aimed to explore the potential influence of climate change and enhanced levels of particulate organic carbon on exposure to neutral organic contaminants in the Arctic environment. While the changes in model output for the atmosphere (boundary layer) are discussed in the paper, the main focus is on how freely-dissolved concentrations in the marine environment respond to the scenarios implemented. This aspect is a key consideration for exposure to neutral organic contaminants given its direct influence on chemical accumulation at the base of the pelagic food web (*e.g.* plankton → zooplankton → Arctic cod → Ringed Seal → Human).

Introduction

The potential influence of global climate change (GCC) on exposure to neutral organic chemicals in both industrialized and remote regions is increasingly gaining the attention of scientists interested in persistent organic pollutants (POPs) and other contaminant issues.[1–10] For example, climate variables are more frequently being used to interpret spatial and temporal patterns in biomonitoring data for POPs, particularly in the Arctic environment which is already experiencing substantial changes (*e.g.* higher temperatures, reduced sea-ice cover).[11–14] These research papers complement past and ongoing efforts to monitor contaminant levels in the Arctic environment and assess exposure of wildlife and humans to organic chemicals.[15–18] The public availability of global and regional-scale projections of climatic conditions throughout the 21st century (*e.g.* changes in surface air temperatures, precipitation rates and atmospheric circulation patterns)[19–22] has also facilitated the application of multimedia environmental fate models to explore some of the potential implications of GCC for contaminant issues.[23–29]

A common strategy adopted for model simulations aiming to explore the potential influence of GCC on the fate and transport of organic chemicals is to define a parameter set representing

[a]*Department of Physical and Environmental Sciences, University of Toronto Scarborough, 1265 Military Trail, Toronto, Ontario, Canada, M1C 1A4. E-mail: james.armitage@utoronto.ca; Fax: +1 416 287 7506; Tel: +1 416 287 7277*

[b]*Department of Occupational Medicine, Aarhus University Hospital, Nørrebrogade 44, Aarhus C, Denmark 8000*

† Electronic supplementary information (ESI) available: Additional details on the GloboPOP model, GCC scenario development and model application. See DOI: 10.1039/c3em00315a

Open Access Article. Published on 18 October 2013. Downloaded on 9/6/2024 8:07:53 AM. This article is licensed under a Creative Commons Attribution 3.0 Unported Licence.

contemporary conditions ('before') and then a modified parameter set incorporating projected changes for a future climate ('after'). Simulations incorporating the temporal trend in projected climate changes over the 21st-century have also been conducted.[28,29] The main focus of most previous modelling studies has been on legacy contaminants such as hexachlorobenzene, polychlorinated biphenyls (PCBs), hexachlorocyclohexanes (HCHs) and polychlorinated dibenzodioxins and furans.[23–30] Modeling these legacy contaminants is useful because (i) POPs are of toxicological concern, (ii) monitoring data are often available to evaluate model performance under contemporary conditions and hence build confidence in the reliability of model output under GCC scenarios and (iii) their physical–chemical properties are also relatively well-known, reducing an important source of model input uncertainty. Excluding changes in emissions, model output under the assumed GCC scenarios is typically less than a factor of two different from model output using contemporary (*i.e.* 20th century) conditions[30] and both positive (*e.g.* reduced contaminant levels) and negative (*e.g.* elevated contaminant levels) outcomes have been reported, depending on the model application and environmental medium being considered (*e.g.* atmosphere *vs.* surface water).

Climate projections indicate that the Arctic environment will experience the greatest warming over the 21st century[19–22] resulting in profound changes to key elements of the ecosystem, particularly the cryosphere (*i.e.* lake and sea-ice, permafrost, glaciers). Primary production is also expected to change in the Arctic environment.[22,31–38] For example, alterations in diatom community structure have already been observed in high Arctic lakes, rationalized primarily in the context of climatic factors such as shorter duration of ice cover, longer growing season, and more favorable thermal stratification patterns.[35–38] A recent satellite-based study[33] conducted at regional-scale over the period 1998–2009 reported a statistically significant increase (+20%) in total annual net primary productivity (NPP) in the Arctic Ocean, predominantly due to increases in both the extent of open water and the duration of the open water season. The main factors controlling primary production in the Arctic Ocean are light limitation (*e.g.* in areas presently covered by multi-year sea ice) and nutrient limitation (particularly in highly stratified waters).[22] Projected changes to primary production in the marine environment are uncertain and region-specific, with estimates ranging from approximately +5–10% to 2–5-fold higher.[22,31–34] All else being equal, enhanced primary production will lead to higher levels of organic carbon (OC) in the water column.[27] Permafrost melt and increased coastal erosion in the Arctic are additional pathways for OC inputs to be influenced by GCC.[39–41]

The link between primary production in aquatic environments, (particulate) organic carbon levels and exposure to hydrophobic organic contaminants is re-emerging as a topic of interest. For example, based on trends in Σhexa- and Σhepta-PCB levels in burbot (*Lota lota*) and sedimentary organic matter over the period 1985–2009, it was recently hypothesized that increased primary production (related to climate change) corresponds to enhanced exposure potential to hydrophobic contaminants.[12] On the other hand, there are numerous studies reporting an inverse relationship between primary production (or particulate organic carbon levels in the water column) and body burdens of hydrophobic chemicals in aquatic organisms.[27,42–46] Concentrations in pelagic biota can be lower in eutrophic systems even if the total amount of chemical in the abiotic environment is higher compared to less productive systems.[45] The implication of eutrophication for benthic infauna depends on how organic carbon normalized concentrations in the active sediment layer are influenced as well as whether respiratory exchange occurs primarily with sediment pore water or overlying water. While organic carbon-normalized concentrations of ΣPCBs in surface sediments showed no relationship with trophic status in a survey of 19 Swedish lakes located in close proximity,[45] these findings cannot be assumed to be universal.

To date, global-scale modeling studies seeking to explore the potential influence of GCC on the fate and transport of organic chemicals have not included changes to organic carbon cycling in the Arctic environment. Accordingly, the main objective of the current study is to explore the potential influence of particulate organic carbon (POC) scenarios on the fate of neutral organic contaminants in combination with other GCC projections. Long-range transport is assumed to be the only source of contaminants entering the Arctic environment. Model output is generated over a 40-year period for hypothetical chemicals covering a range of partitioning properties (*i.e.* air–water partition coefficient, K_{AW}; octanol–water partition coefficient, K_{OW}; octanol–air partition coefficient, K_{OA}) and susceptibility to degradation in the environment. The modeling approach is evaluative in nature but still provides useful insights into the potential influence of GCC scenarios on the behaviour of organic contaminants in the environment. As exposure to organic contaminants in the Arctic *via* the marine food web remains a particular concern,[47,48] the results are discussed primarily in the context of exposure to neutral organic contaminants in the marine environment.

Materials and methods

Global-scale fate and transport model (GloboPOP)

All simulations were conducted with the GloboPOP model,[49,50] a fugacity-based chemical fate and transport model. Important features of this model are presented in Section S1 of the ESI.† The globe is divided into ten latitudinal bands, each with well-mixed compartments representing the atmosphere (four layers), surface ocean water (0–200 m depth) and the terrestrial environment which includes freshwater and underlying sediments, different soil types (*e.g.* agricultural, uncultivated, forest) and forest canopies (deciduous, coniferous). Seasonal snow packs are included in the North Temperature, North Boreal and North Polar zones (ESI, Section S1†) whereas the South Polar zone has a permanent snow pack. Sea-ice cover (% of water surface area covered) is tracked for the North Polar, South Polar and South Sub-Polar zones. Details on the treatment of snow (as precipitation and snow pack) and other recent modifications to the model are presented elsewhere.[51] One advantage of using

 This journal is © The Royal Society of Chemistry 2013

Open Access Article. Published on 18 October 2013. Downloaded on 9/6/2024 8:07:53 AM.
This article is licensed under a Creative Commons Attribution 3.0 Unported Licence.

the current version of GloboPOP is that shelf sediments in the Arctic Ocean are explicitly included. This compartment is an important reservoir of hydrophobic organic contaminants in the Arctic environment and can act as major secondary source once primary emissions are exhausted.[51]

Global climate change (GCC) scenarios

The GCC scenarios implemented for the current study reflect changes in (i) air and ocean water temperatures, (ii) precipitation rates, and (iii) seasonal sea-ice cover (and ice-free periods for freshwater systems). General features of the GCC scenarios are summarized in Table 1 whereas specific details are presented in Section S2 of the ESI.† Given the coarse spatial resolution of the model and limited influence reported in previous global-scale modeling exercises,[26,29] projected changes to atmospheric and oceanic circulation patterns are not considered. Note that all changes related to the GCC scenarios are introduced at the beginning of the simulation as opposed to being introduced incrementally over time. The default parameterization scenario is based on the original model[49] and recent updates[50,51] whereas the GCC scenarios are defined using regional and global-scale projections for climate change in the latter part of the 21st century.[19–22]

Particulate organic carbon (POC) scenarios

Levels of particulate organic carbon (POC) in surface ocean waters vary substantially in different regions of the Arctic Ocean due to factors such as the intensity and duration of primary production, distance from shore/intensity of inputs from terrestrial sources (*e.g.* riverine inflow, coastal erosion) and the potential for resuspension from underlying sediment beds.[52] This variability is reflected in the ranges of values for POC levels in surface waters reported for a recent sampling campaign (ISSS-08 Cruise).[53] For example, measured ranges were 6.5–17.8 μM in the Barents Sea, 3.4–33.0 μM in the Kara Sea, 1.2–151.9 μM in the Laptev Sea, 1.0–19.4 μM in the W-East Siberian Sea, 2.0–36.6 μM in the E-East Siberian Sea and 3.1–33.1 μM in the Chukchi Sea. Measured values from other studies range from approximately 10–30 μM in the Barents Sea,[54] 1–10 μM in the Canada Basin[55,56] and <1 μM reported for the central Arctic.[57] As the coarse spatial resolution of the GloboPOP model does not allow regional differences in POC levels to be represented, simulations for the default GloboPOP simulations and the GCC scenarios (Table 1) were conducted assuming average POC levels in Arctic surface waters of 20 μg L^{-1} (~1.5 μM) and 200 μg L^{-1} (~15 μM).

Changes in primary production (PP) projected for the Arctic Ocean described in the Arctic Climate Impact Assessment (ACIA)[22] are as follows; (i) light-limited regions: increased 2–5-fold, due to sea-ice disappearance, assuming no nutrient limitation; (ii) Barents Sea: increased ≥2-fold due to deeper wind-mixed layer and supply of nutrients from underlying Atlantic water; (iii) Arctic shelf seas: increased ≥2-fold due to retreat of permanent ice pack beyond shelf break and subsequent onset of enhanced upwelling and exchange with nutrient-rich offshore waters. Recent studies incorporating model simulations suggest far more modest changes. For example, Ellingsen *et al.*[31] applied a coupled hydrodynamic-ecological model for the Barents Sea and reported only an 8% increase in PP over the next 65 years. Similarly, Lavoie *et al.*[32] employed a coupled sea ice-ocean-biological 1D model to project future PP

Table 1 Summary of the GCC scenario parameterization implemented for the current study compared to the default GloboPOP parameterization[a]

GCC scenario	Parameterization	Details (see ESI)
GCC	*Direct*	
	(i) Altered temperatures in atmosphere/ terrestrial environment and surface ocean (up to + 8–10 °C in Arctic, +3–4 °C elsewhere)	Table S1–S3
	(ii) Altered precipitation rates (up to ±35%)	Table S4 and S5
	Indirect	
	(i) Altered run-off volumes (linked to precipitation rate)	—
	(ii) ↑ ice-free period of freshwater (N.Temperate, N.Boreal, N.Polar)	+35 to 55 days
	(iii) ↓ sea-ice cover, Arctic Ocean (N.Polar)	Fig. S1
	(iv) Altered snow pack accumulation (linked to precipitation rate)	Fig. S2
	(v) ↓ snow pack melt period in Spring	−10 days
GCC + OC	GCC (see above)+	ESI, Section S2
	(i) ↑ volume fraction of POC in surface ocean water[b]	×2.5
	(ii) ↑ SOC content of Arctic Ocean shelf sediments	×2.5
	(iii) ↑ volume fraction of POC in Arctic freshwater system[b]	×1.5
	(iv) ↑ SOC content of freshwater sediments	×1.5

[a] POC = particulate organic carbon; SOC = sediment organic carbon. [b] Mass transfer coefficient for deposition (*i.e.* settling) of particle-bound contaminant in freshwater and marine compartment increased by the same factor.

Open Access Article. Published on 18 October 2013. Downloaded on 9/6/2024 8:07:53 AM.
This article is licensed under a Creative Commons Attribution 3.0 Unported Licence.

for the Mackenzie Shelf (Beaufort Sea); projected increases in average annual primary production are low (increased 6 and 9% for 2050 and 2090 respectively *vs.* present day), primarily due to the influence of enhanced fresh water input (intensified stratification, reduced replenishment of nutrients). On the other hand, as noted above, a statistically significant increase (+20%) in total annual net primary productivity (NPP) in the Arctic Ocean has already been reported for the period 1998–2009.[33] While primary productivity per unit area per unit time is similar, total annual NPP increased because both area for primary production and growth period have increased. Assuming no nutrient limitations, the authors suggested that total annual NPP could increase nearly 2-fold by mid-century, when summer minimum ice coverage approaches zero. In agreement with this estimation, Slagstad *et al.*[34] reported increases in gross and net primary productivity in the range of approximately 1.1–4-fold based on model simulations of different regions of the Arctic Ocean assuming ice-free conditions in summer.

Based on the considerations presented above, the volume fraction of POC in the water column of the Arctic surface ocean was increased 2.5-fold in the GCC + OC scenario. In other words, the default values for the concentration of POC in the water column (C_{POC}) are multiplied by a factor of 2.5 (*i.e.* $C_{POC} = 50$ and 500 μg L^{-1}). To be consistent with this change, the mass transport coefficient (MTC) characterizing deposition (*i.e.* settling) of particle-bound contaminant was increased by the same factor. Additionally, the organic carbon content of the shelf sediments (SOC) was also increased 2.5-fold. Changes in the parameterization of the freshwater compartment (see Table 1) are discussed briefly in the ESI (Section S2†).

Model application

A total of six scenarios were simulated for the current study (see Table 1 and ESI Section S2†). Simulations were first conducted using the default climate parameterization assuming a C_{POC} in the Arctic Ocean surface water of 20 μg L^{-1} (see above). The simulations were then repeated assuming a C_{POC} of 200 μg L^{-1}. Model outputs were then generated for the GCC scenario (Table 1) under the same two assumptions regarding POC (and SOC) in the Arctic environment. Next, model output was generated for the GCC + OC scenario (Table 1), where, for example, concentrations of POC in the Arctic Ocean surface water are 2.5-fold higher (*i.e.* C_{POC} = 50 μg L^{-1} and then 500 μg L^{-1}). For each scenario, the model was run for a set of hypothetical chemicals covering a wide range of partitioning property values (log K_{OA} = 4 to 15, log K_{AW} = 3 to −5 where log K_{OW} = log K_{OA} − log K_{AW} and only log K_{OW} values from 1 to 12 are included). All chemicals were assumed to be relatively persistent in the environment and degrade with the following characteristics; (i) a second-order reaction rate constant with atmospheric OH radicals (k_{OH}) at 25 °C of 1×10^{-12} cm^3 per molecule per s and (ii) degradation half-lives at 25 °C of 1, 2 and 10 years in water (fresh, marine), soils (all types) and sediments (fresh, marine) respectively. Degradation half-lives in snow pack and forest canopies were assumed to be equal to those in water. All simulations were repeated assuming 10-fold slower reaction kinetics, *i.e.* a k_{OH} at 25 °C of 1×10^{-13} cm^3 per molecule per s and degradation half-lives at 25 °C of 10, 20 and 100 years in water (marine), soils (all types) and sediments. Taken together, this range of degradation half-lives is representative of many POPs. Note that the two k_{OH} values listed above correspond to a degradation half-life in the atmosphere of approximately 8 and 80 days respectively at 25 °C, assuming a global average atmospheric OH radical concentration[58] of 9.8×10^5 molecules cm^{-3}. However, atmospheric degradation half-lives in each model zone are determined on a daily basis following the seasonal patterns in temperature and OH radical concentrations. Assumptions regarding the temperature-dependence of the partitioning constants and degradation kinetics are presented in Section S3 of the ESI.†

All chemicals were emitted into the environment using the same 40-year emission scenario which specifies a constant (unit) emission rate for 20 years followed by zero emissions for the remaining 20 years. This approach allows model output to be generated and compared during the primary emission phase (Year 0–20) and as secondary sources (*e.g.* environmental reservoirs such as boreal forest soils) come to dominate (Year 20–40). Over the latter period, levels in the environment are declining due to degradation and export out of the model domain (*e.g.* sediment burial, export to deep oceans). The rate at which levels dissipate is specific to the environmental compartment and model zone however. Emissions were directed 100% to the atmosphere and the spatial distribution of emissions is based on estimates for PCBs.[59] This pattern is assumed to represent a typical industrial chemical (*i.e.* emitted predominantly in the northern Hemisphere at mid-latitudes) (see Section S4 of the ESI†). Emissions to the North Polar zone of the model were purposely set to zero to ensure that all mass entering the Arctic environment is due to long-range transport. The model calculations are solved numerically with a time step ranging from 1–12 h, depending on the partitioning properties of the hypothetical chemical.

Assessment metrics

The assessment of the potential influence of GCC scenarios on the behavior of neutral organic contaminants in the Arctic environment during the primary emission phase is based on the values of the following metrics at Year 20, (i) Arctic Contamination Potential ($eACP_{20}$),[60] (ii) average concentration in the surface layer of the atmosphere (C_A) and (iii) average freely-dissolved concentration in the surface ocean (C_O). $eACP_{20}$ is calculated from the model output as:

$$eACP_{20} = \frac{(M_T - M_A)}{E_G} \quad (1)$$

where M_T is the total mass of chemical in the North Polar zone of the model, M_A is the total mass of chemical in the atmosphere of the North Polar zone and E_G is the total mass of chemical emitted to the global environment. Model output from all GCC scenarios (Table 1) is compared to default model output for each partitioning property combination and then the

 This journal is © The Royal Society of Chemistry 2013

Open Access Article. Published on 18 October 2013. Downloaded on 9/6/2024 8:07:53 AM.
This article is licensed under a Creative Commons Attribution 3.0 Unported Licence.

ratios (*i.e.*, GCC:Default, GCC + OC:Default) displayed as a function of log K_{OA} and log K_{AW}. Ratios greater than one mean that the GCC scenario has resulted in elevated contamination of the Arctic environment compared to the default scenario. We chose to focus on $eACP_{20}$, C_A and C_O because these outputs represent long-range transport potential, a frequently sampled abiotic medium in the Arctic and the most relevant consideration for exposure to contaminants *via* the marine pelagic food web (*e.g.* water → phytoplankton → zooplankton → Arctic cod → ringed seal → human/polar bear) respectively. Patterns of response in the atmosphere are also of interest because atmospheric concentrations of some POPs in the Arctic (*e.g.* HCHs) have already been suggested to be responding to climate forcings.[61] Priority is given to the marine pelagic food web because consumption of seal blubber is associated with elevated body burdens of POPs in top predators (*i.e.* humans and polar bears).[15,16]

A different metric is used to assess the potential influence of GCC scenarios on the fate of neutral organic contaminants in the Arctic environment after primary emissions have ceased. In this case, the ratio between model output at Year 40 and Year 20 for each scenario is calculated (R) and then the assessment metric (M_{40}) is based on the comparison between the Year 40 : 20 ratios for the GCC and default scenarios, *e.g.*

$$R_{DEF} = \frac{C_{A,40,DEF}}{C_{A,20,DEF}}, R_{GCC} = \frac{C_{A,40,GCC}}{C_{A,20,GCC}} \text{ and } M_{40} = \frac{R_{GCC}}{R_{DEF}} \quad (2)$$

where $C_{A,40,DEF\text{ or }GCC}$ is the average surface air concentration at Year 40 and $C_{A,20,DEF\text{ or }GCC}$ is the average surface air concentration at Year 20. This approach was adopted because the current study does not sequentially introduce changes in model parameterization during the simulation and the modeled concentrations (and masses) at Year 20 are not identical between the different scenarios. The M_{40} values are surrogates for apparent dissipation half-life and values greater than one mean that the GCC scenario has resulted in a slower rate of depuration compared to the default scenario (*e.g.* the time required to reduce ambient concentrations in the Arctic environment by a factor of two is longer). Other interpretations of this assessment metric are discussed in the following section. An illustration of the temporal trend in emissions, representative model outputs under default and GCC scenarios and how model output at Year 20 and 40 is used to generate the assessment metrics is presented in Fig. 1. Note that the metrics at Year 20 and Year 40 are not directly comparable in terms of the magnitude of change. All results of the present set of model simulations are considered evaluative in nature (*i.e.* best suited to explore sensitivities and trends at a screening level).

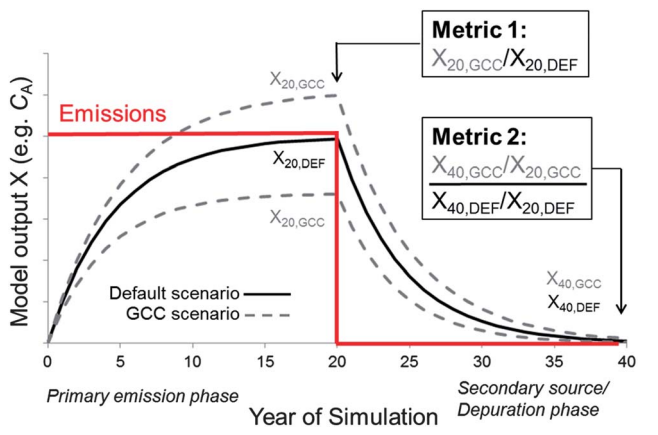

Fig. 1 Plot illustrating the temporal trend of the emission scenario, representative model outputs under default and GCC scenarios and how model output at Year 20 and 40 is used to generate the assessment metrics. The solid line represents model output under the default parameterization. The dotted lines represent model output under the GCC scenarios (which can result in higher or lower values compared to the default scenario, depending on the chemical properties).

Results and discussion

Primary emissions phase (Year 0–20)

A comparison of model output from the GCC scenarios (GCC, GCC + OC) to the default scenario in Year 20 for the selected model outputs ($eACP_{20}$, C_A, C_O) is presented in Fig. 2. These results are for the scenarios assuming default POC concentrations in Arctic Ocean surface water of 200 μg L^{-1}. A comparison of the default and GCC + OC scenario assuming POC levels of 20 μg L^{-1} is presented in Section S5 of the ESI.† All model outputs presented in Fig. 2 were generated assuming the longer degradation half-lives (*i.e.* slower degradation rates, see above). Results obtained using the shorter degradation half-lives are broadly similar to those shown in Fig. 2 and hence are not discussed further. The general patterns in long-range transport potential and accumulation in the Arctic environment for the hypothetical chemicals considered are summarized in Section S6 of the ESI.†

Key features of the results presented in Fig. 2 are as follows. First, regardless of the model output considered, the changes caused by implementation of the GCC scenarios (Table 1) typically result in values within a factor of two of the default scenario. For example, the Arctic Contamination Potential ($eACP_{20}$) is relatively insensitive to both GCC scenarios across a wide range of partitioning property combinations, exhibiting changes in the range of ±20%. Such results stem from the fact that changes implemented for the GCC scenarios can act antagonistically (*i.e.* influences are competing and so tend to balance out). Furthermore, some changes implemented in the GCC scenarios (*e.g.* precipitation rates) are limited in magnitude. The $eACP_{20}$s of volatile chemicals (log $K_{AW} \geq 1$) with log $K_{OA} \leq 7$ are more sensitive to the GCC scenarios (*i.e.* values reduced to 50% or less of default model output) but such chemicals tend to distribute into the gas phase in the atmosphere with only a relatively small fraction present in surface media (ESI, Section S6†). Higher temperatures under the GCC scenarios are particularly effective in reducing net deposition for these chemicals, partly because of the non-linear relationship between temperature and partitioning property values.

Secondly, increases in average air concentration in Year 20 (up to +40%) are observed under both GCC scenarios for chemicals with log $K_{AW} \geq -4.5$ and log K_{OA} between approximately 7 and 10.5. This behaviour reflects alterations in long-range transport efficiency of such contaminants to the Arctic

Open Access Article. Published on 18 October 2013. Downloaded on 9/6/2024 8:07:53 AM.
This article is licensed under a Creative Commons Attribution 3.0 Unported Licence.

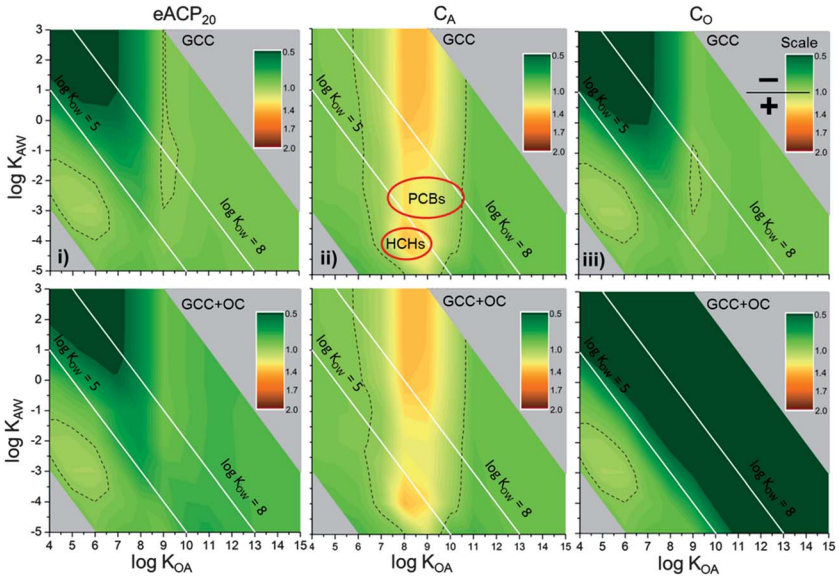

Fig. 2 Comparison of model output from the GCC scenarios (GCC, GCC + OC) to the default scenario in Year 20 for (i) Arctic Contamination Potential ($eACP_{20}$), (ii) average concentration in surface air (C_A) and (iii) average freely-dissolved concentration in surface ocean water (C_O). Ratios greater than 1.0 (+) mean that model output under the GCC scenario is higher than output from the default scenario. The dotted line indicates a transition from ratios less than 1.0 to those greater than 1.0. The approximate regions of chemical partitioning space occupied by PCBs and HCHs are also indicated (see GCC, C_A panel).

environment and changes in the net deposition fluxes and accumulation in surface media (*e.g.* soils and shelf sediments). Note that this range of partitioning properties overlaps with known POPs such as PCBs. The suggestion that atmospheric concentrations of chemicals with such partitioning properties may increase in direct response to higher air temperatures is consistent with previous global-scale modeling studies.[26,29] However, it is also clear that the responses to the GCC scenarios seen in the surface compartments are different from the responses seen in the atmosphere (*e.g.* compare the $eACP_{20}$ and C_O plots for the GCC scenario to the output for C_A in Fig. 2). Accordingly, the direction (and magnitude) of the response to GCC scenarios predicted for the atmosphere cannot be used to predict responses in other compartments or speculate directly on the implications for exposure to organic contaminants *via* dietary uptake.

The most important feature of the results presented in Fig. 2 in the context of exposure to neutral organic contaminants is that C_O is reduced over a much wider range of partitioning property combinations in the GCC + OC scenario compared to the GCC scenario. For chemicals with $\log K_{OW} \geq 5.5$ and $\log K_{OA} > 7$, the response is roughly in proportion to the extent that the volume fraction of POC in the water column is assumed to increase in the GCC + OC scenario (*i.e.*, a factor of 2.5; Table 1). The model output for C_O is driven by a mass dilution effect (*i.e.* as the volume of particulate OC is increased, less chemical mass is present in the dissolved phase) as well as enhanced deposition of particulate-bound chemical out of the surface water to the shelf sediments and deep ocean. While atmospheric deposition becomes more favorable thermodynamically, such inputs are not sufficient to counter the enhanced losses associated with particle settling and consequently, OC-normalized concentrations in suspended solids are also reduced. These results are consistent with past studies on the influence of eutrophication and contaminant dynamics in aquatic systems[42–45] and also with recent empirical data characterizing the temporal trends in bioaccumulation associated with the rapid changes in primary production observed in an alpine lake.[46] The decrease in C_O is expected to lead to a concomitant reduction in exposure at the base of the pelagic food web, which then propagates upwards.[27] It is also worth noting that organic carbon-normalized concentrations in the shelf sediments of the Arctic Ocean (active layer only, *i.e.* top 5 cm) are reduced in the GCC + OC scenario across a similar range of partitioning properties that exhibit reduced freely-dissolved concentrations (results not shown). Lower organic carbon-normalized concentrations in the shelf sediments imply reduced exposure potential in benthic organisms *via* respiration of pore-water and ingestion of sediment OC. As shown in the ESI (Section S5†), the comparison between the default model output assuming $C_{POC} = 20\ \mu g\ L^{-1}$ and the GCC + OC scenario is broadly similar to the results shown in Fig. 2 (default $C_{POC} = 200\ \mu g\ L^{-1}$). However, a shift occurs in the threshold of response for chemicals with $\log K_{OW}$ between 5 and 8 and $\log K_{AW} < -1$. Essentially, when the default POC concentrations are reduced 10-fold, K_{OW} must be increased 10-fold to achieve the same reduction in freely-dissolved water concentration. Because of the heterogeneity in POC levels in the Arctic Ocean, the implication of these findings is that changes in the exposure potential for hydrophobic chemicals may not be uniform across the region, even given the same proportional change in POC levels.

Secondary source/depuration phase (Year 20–40)

A comparison of model output from the GCC scenarios (GCC, GCC + OC) to the default scenario in Year 40 *versus* Year 20 (see

 This journal is © The Royal Society of Chemistry 2013

Open Access Article. Published on 18 October 2013. Downloaded on 9/6/2024 8:07:53 AM.
This article is licensed under a Creative Commons Attribution 3.0 Unported Licence.

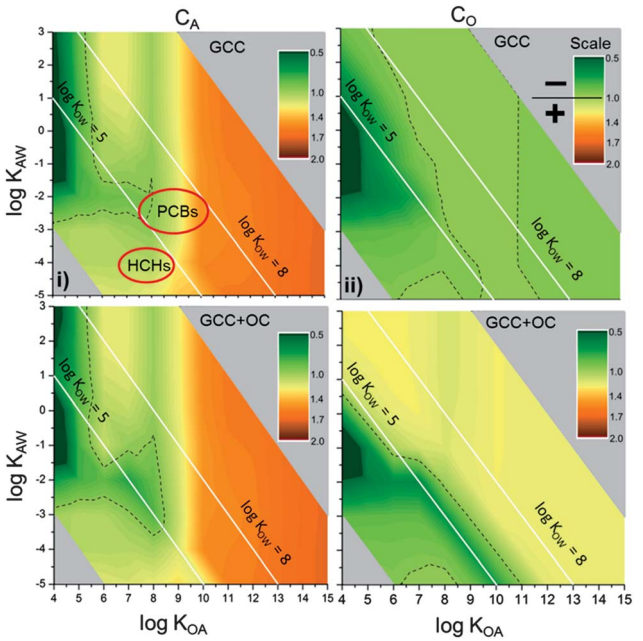

Fig. 3 Comparison of model output from the GCC scenarios (GCC, GCC + OC) to the default scenario in Year 40 *versus* Year 20 for (i) average concentration in surface air (C_A) and (ii) average freely-dissolved concentration in surface ocean water (C_O). Ratios greater than 1.0 (+) mean that the apparent dissipation half-life is greater in the GCC scenario than the default scenario. The dotted line indicates the transition from ratios less than 1.0 to those greater than 1.0. The approximate regions of chemical partitioning space occupied by PCBs and HCHs are also indicated (see GCC, C_A panel).

eqn (2)) for average concentration in surface air (C_A) and average freely-dissolved concentration in surface ocean water (C_O) is presented in Fig. 3. These comparisons represent the changes in the apparent dissipation half-life of the chemical from the Arctic environment as a whole and in the atmospheric boundary layer and surface ocean water. As in Fig. 2, all model outputs presented in Fig. 3 were generated assuming the longer degradation half-lives. Also, as before, results obtained using the shorter degradation half-lives are broadly similar to those shown in Fig. 3 and are not explicitly discussed.

The most obvious feature of the results presented in Fig. 3 is that the apparent dissipation half-life in the atmospheric boundary layer (C_A) is greater under the GCC scenarios compared to the default conditions (*i.e.* ratio greater than one; see eqn (2)) across a wide range of partitioning property combinations. For all such chemicals, the reduction in air concentrations is lower *in relative terms* over the last 20 years of the simulation. The highest sensitivity in the atmospheric boundary layer (C_A) under the GCC scenarios is seen for chemicals with log K_{OA} > 10.5. Enhanced revolatilization from secondary sources is an important factor driving the results for such chemicals. This phenomenon is also important for other partitioning property combinations, including those overlapping known POPs. The results follow intuitively from the higher temperatures and reduced period of time that transport from soils and the surface ocean water to the atmosphere is impeded by snow pack and sea-ice respectively in the GCC scenarios. There are no important differences between the GCC and GCC + OC scenarios. The influence of the GCC scenarios on temporal trends in atmospheric levels during the depuration phase (Year 20–40) is consistent with a recent analysis of POP air monitoring data from the Arctic (*i.e.* slowing decline in atmospheric levels due to enhanced inputs from secondary reservoirs).[61] However, the changes implemented in the GCC scenarios are more extreme than the changes observed in the Arctic environment to date (*e.g.* sea-ice cover reduced to negligible fraction of Arctic Ocean in the GCC scenarios) and hence the model results should not be over-interpreted when discussing trends in contemporary monitoring data.

The other feature of the results presented in Fig. 3 worth discussing is that response patterns observed in the atmosphere (C_A) are different from the pattern of those observed in the freely-dissolved concentrations in surface ocean water (C_O). Furthermore, the responses in C_O are substantially different between the GCC and GCC + OC scenarios for chemicals with log $K_{OW} \geq 5$. Generally speaking, the increases in the apparent dissipation half-lives in GCC + OC scenario are more pronounced (*i.e.* higher sensitivity). The direction of the response in the C_O metric in the depuration phase (Fig. 3) is also opposite to what was observed during the primary emission phase (Fig. 2). These patterns can be explained by considering the relative importance of sediment resuspension as a source term for the surface ocean over the simulation period. During the primary emission phase (Year 0–20), atmospheric deposition is more important than sediment resuspension in terms of driving levels in the surface ocean and hence alterations in sediment-water exchange (*i.e.* enhanced mass transfer coefficient, MTC, for particulate deposition) are not influential. However, resuspension from shelf sediments increasingly dominates after Year 20 and hence assumptions regarding the MTCs for sediment deposition, resuspension and burial become important. In these simulations, sediment resuspension is assumed to be a constant fraction of the sediment deposition flux and therefore any increase in the sediment deposition MTC (Table 1) is matched by a proportional increase in the resuspension MTC (*i.e.* shelf sediments are more efficient at resupplying the water column in the GCC + OC scenario). The greater apparent dissipation half-lives seen in the surface ocean water are primarily due to this model parameterization approach. Such a response is plausible in reality though, if, for example, enhanced inputs in the water column gradually lead to enhanced OC content in sediments and resuspended particles (*i.e.* more chemical could be delivered to the overlying water column per unit time). Although these results imply that declines from peak exposure levels in the pelagic food web are delayed as a consequence of GCC, no specific comments on the toxicological implications can be made given the generic nature of the current model application.

Limitations and future considerations

The results presented in Fig. 2 and 3 are broadly consistent with expectations based on previous global-scale modeling characterizing the potential direct influence of GCC on chemical fate and transport[26,29,30] in terms of magnitude of response. These

Open Access Article. Published on 18 October 2013. Downloaded on 9/6/2024 8:07:53 AM. This article is licensed under a Creative Commons Attribution 3.0 Unported Licence.

results lend support to the assertion that indirect effects and behavioural responses to GCC (*e.g.* dietary shifts, northward shifts in industrial or agricultural activity) may be more important considerations overall compared to direct effects of GCC.[10,30] However, it is also important to recognize the limitations inherent to the evaluative modeling approach employed and the scope of the GCC scenarios considered in the present study. For example, potential GCC-related changes in emission strength and spatial distribution over time and the response to GCC scenarios of chemicals exhibiting different modes of entry into the environment (*e.g.* for a pesticide emitted 95% emission to soil, 5% to freshwater as opposed to 100% to the air) were not simulated. The simulations in the present study were also conducted using degradation half-lives and activation energies typical of most known POPs and hence are not broadly representative of the entire realm of chemical space. Some of these aspects were explored in a recent global-scale modeling exercise.[29] As the global fate of chemicals with lower environmental persistence than assumed here increasingly becomes dominated by degradation kinetics, higher temperatures under GCC scenarios increasingly result in reduced exposure potential relative to the default scenario (*i.e.* as T increases, mass of chemical in environment decreases).[29] As the selected emission pattern (mode of entry, spatial distribution) and temperature-dependencies of partitioning properties and reactivity are most representative of industrial chemicals like PCBs, caution is necessary when extrapolating the results to chemicals that deviate substantially from these assumptions.

It is also worth reiterating that changes in atmospheric and oceanic circulation patterns were not considered in the present study. While changes in long-term (average) atmospheric circulation patterns do not appear to have an important influence on long-range transport potential,[26,29] there are still valid reasons to explore these aspects using more appropriate (*i.e.* spatially-resolved) tools. For example, the potential implications of changes in the frequency and intensity of positive NAO events (NAO+), conditions which favour long-range transport of chemicals to the Arctic from European and North American sources,[24,62] could be simulated. The potential short-term and long-term influence of altered frequencies of episodic transport events and extreme weather conditions could also be assessed. Finally, although the available empirical data do not generally support the hypothesis that sea-ice is an important mass reservoir and transport pathway for the organic compounds studied to date or that food webs intimately linked with sea-ice (*i.e.* including epontic organisms) have higher exposure potential than other pelagic food webs,[63–65] a more detailed treatment of this compartment in the model is required to fully assess the potential implications of GCC for exposure in the Arctic environment. The role of glacier melt in the Arctic (*e.g.* input of stored chemical *vs.* dilution through melt of pre-industrial ice) also requires further consideration.[2,30]

Conclusions

The different model results seen in the atmospheric boundary layer (C_A) compared to the surface ocean (C_O) demonstrate that responses to GCC are best evaluated from a multimedia perspective, ideally using the most exposure-relevant metrics (*e.g.* freely-dissolved as opposed to total water concentrations, organic carbon-normalized as opposed to total sediment concentrations). The differences in model output between the GCC and GCC + OC scenarios illustrate that enhanced particulate OC in the Arctic marine environment may be one of the more important considerations for hydrophobic chemicals. During the primary emission phase, enhanced POC in the Arctic marine environment can exert a mitigating influence on exposure to hydrophobic chemicals. Potential changes in POC cycling and sediment-water exchange dynamics linked to GCC are therefore key processes to consider further, particularly in the context of determining if responses in pelagic food webs are representative of responses in benthos (*e.g.* benthic infauna inhabiting shelf sediments). Unfortunately, projecting changes to inputs of organic carbon to the Arctic environment due to enhanced primary production, permafrost melt, coastal erosion and other alterations to organic carbon cycling is challenging and subject to many data gaps.[66] In addition to requiring an estimation of the volume of organic material involved (and the spatial and temporal variability), other aspects to consider include relative sorption capacity of organic carbon released from permafrost and eroding coastlines (compared to planktonic/algal OC) and the extent to which enhanced delivery or production of particulate OC may be offset by enhanced microbial degradation in the water column.[67–70] For example, the extent to which mineralization of POC occurs in the water column was hypothesized to exert an important influence on how chemicals distribute between suspended solids, sediments and water.[71] For legacy pollutants such as PCBs, the contaminant levels associated with terrestrial OC sources in the Arctic may also be important consideration. Examples of research that could provide useful insights in this context include (i) contaminant concentration *vs.* depth profiles and sorption/desorption experiments with permafrost and eroded coastline soils/sediments, (ii) characterization of the susceptibility to degradation of various organic carbon sources in the Arctic environment and (iii) development and implementation of an improved parameterization of the organic carbon mass balance in the Arctic Ocean for contemporary and potential conditions in the future. More explicit treatment of the fate of organic carbon in shelf sediments is also worth considering. Given the many uncertainties related to the potential for enhanced levels of OC in the Arctic marine environment to influence exposure to neutral organic chemicals, further empirical studies and model development aimed to clarify these aspects are warranted.

Acknowledgements

The EU FP7 project CLEAR (FP7-ENV-2008-1, Grant Agreement no. 226217), the Northern Contaminants Program of Aboriginal Affairs and Northern Development Canada and the Natural

Open Access Article. Published on 18 October 2013. Downloaded on 9/6/2024 8:07:53 AM. This article is licensed under a Creative Commons Attribution 3.0 Unported Licence.

Sciences and Engineering Research Council of Canada are acknowledged for funding support.

References

1 R. W. Macdonald, D. Mackay, Y. F. Li and B. Hickie, *Hum. Ecol. Risk. Assess.*, 2003, **9**, 643–660.
2 R. W. Macdonald, T. Harner and J. Fyfe, *Sci. Total Environ.*, 2005, **342**, 5–86.
3 L. D. Kraemer, J. E. Berner and C. M. Furgal, *Int. J. Circumpolar Health*, 2005, **64**, 498–508.
4 B. M. Jenssen, *Environ. Health Perspect.*, 2006, **114**(S1), 76–80.
5 D. Schiedek, B. Sundelin, J. W. Readman and R. W. Macdonald, *Mar. Pollut. Bull.*, 2007, **54**, 1845–1856.
6 L. Lamon, M. Dalla Valle, A. Critto and A. Marcomini, *Environ. Pollut.*, 2009, **156**, 1971–1980.
7 United Nations Environment Program (UNEP)/Arctic Monitoring and Assessment Program (AMAP), Climate change and POPs: Predicting the Impacts, Report of the UNEP/AMAP Expert Group, Secretariat of the Stockholn Convention, Geneva, 2011, p. 62.
8 G. A. Stern, R. W. Macdonald, P. M. Outridge, S. Wilson, J. Chételat, A. Cole, H. Hintelmann, L. L. Loseto, A. Steffen, F. Wang and C. Zdanowicz, *Sci. Total Environ.*, 2012, **414**, 22–42.
9 R. Kallenborn, C. Halsall, M. Dellong and P. Carlsson, *J. Environ. Monit.*, 2012, **14**, 2854–2869.
10 T. Gouin, J. M. Armitage, I. T. Cousins, D. C. G. Muir, C. A. Ng, L. Reid and S. Tao, *Environ. Toxicol. Chem.*, 2013, **32**, 20–31.
11 M. A. McKinney, E. Peacock and R. J. Letcher, *Environ. Sci. Technol.*, 2009, **43**, 4334–4339.
12 J. Carrie, F. Wang, H. Sanei, R. W. Macdonald, P. M. Outridge and G. A. Stern, *Environ. Sci. Technol.*, 2010, **44**, 316–322.
13 F. Rigét, K. Vorkamp and D. Muir, *J. Environ. Monit.*, 2010, **12**, 2252–2258.
14 J. O. Bustnes, G. W. Gabrielsen and J. Verreault, *Environ. Sci. Technol.*, 2010, **44**, 3155–3161.
15 Arctic Monitoring and Assessment Programme (AMAP), AMAP Assessment Report: Arctic Pollution Issues, Arctic Monitoring and Assessment Programme (AMAP), Oslo, Norway, 1998.
16 Arctic Monitoring and Assessment Programme (AMAP), Arctic Pollution 2009, Arctic Monitoring and Assessment Programme (AMAP), Oslo, Norway, 2009.
17 D. C. G. Muir and C. A. de Wit, *Sci. Total Environ.*, 2010, **408**, 3044–3051.
18 L. Hoferkamp, M. H. Hermanson and D. C. G. Muir, *Sci. Total Environ.*, 2010, **408**, 2985–2994.
19 Intergovernmental Panel on Climate Change (IPCC): Climate Change 2007: Synthesis Report, Contribution of Working Group I, II and III to the Fourth Assessment Report of the Intergovernmental Panel on Climate Change, 2007, http://www.ipcc.ch.
20 Intergovernmental Panel on Climate Change (IPCC): Climate Change 2007: The Physical Science Basis. Contribution of Working Group I to the Fourth Assessment Report of the Intergovernmental Panel on Climate Change, 2007, http://www.ipcc.ch.
21 J. H. Christensen, A. Hewitson, A. Busuioc, A. Chen, X. Gao, I. Held, R. Jones, R. K. Kolli, W.-T. Kwon, R. Laprise, V. M. Rueda, L. Mearns, C. G. Menéndez, A. Räisänen, A. Rinke, A. Sarr and P. Whetton, Regional Climate Projections, in *Climate Change: The Physical Science Basis. Contribution of Working Group 1 to the Fourth Assessment Report of the Intergovernmental Panel on Climate Change*, Cambridge University Press, Cambridge, United Kingdom and New York, NY, USA, 2007.
22 Arctic Climate Impact Assessment (ACIA), Cambridge University Press, 2005, http://www.acia.uaf.edu.
23 T. E. McKone, J. I. Daniels and M. Goldman, *Risk Analysis*, 1996, **16**, 377–393.
24 M. MacLeod, W. J. Riley and T. E. McKone, *Environ. Sci. Technol.*, 2005, **39**, 6749–6756.
25 M. Dalla Valle, E. Codato and A. Marcomini, *Chemosphere*, 2007, **67**, 1287–1295.
26 L. Lamon, H. von Waldow, M. MacLeod, M. Scheringer, A. Marcomini and K. Hungerbühler, *Environ. Sci. Technol.*, 2009, **43**, 5818–5824.
27 K. Borgå, T. M. Saloranta and A. Ruus, *Environ. Toxicol. Chem.*, 2010, **29**, 1349–1357.
28 J. Ma and Z. Cao, *Environ. Sci. Technol.*, 2010, **44**, 8567–8573.
29 H. Wöhrnschimmel, M. MacLeod and K. Hungerbühler, *Environ. Sci. Technol.*, 2013, **47**, 2323–2330.
30 J. M. Armitage, C. L. Quinn and F. Wania, *J. Environ. Monit.*, 2011, **13**, 1532–1546.
31 I. H. Ellingsen, P. Dalpadado, D. Slagstad and H. Loeng, *Clim. Change*, 2008, **87**, 155–175.
32 D. Lavoie, K. L. Denman and R. W. Macdonald, *J. Geophys. Res.*, 2010, **115**, C04018, DOI: 10.1029/2009JC005493.
33 K. R. Arrigo and G. L. van Dijken, *J. Geophys. Res.*, 2011, **116**, C09011, DOI: 10.1029/2011JC007151.
34 D. Slagstad, I. H. Ellingsen and P. Wassmann, *Prog. Oceanogr.*, 2011, **90**, 117–131.
35 K. Rühland, A. Priesnitz and J. P. Smol, *Arct. Ant. Alp. Res.*, 2003, **35**, 110–123.
36 B. B. Perren, R. S. Bradley and P. Francus, *Arct. Ant. Alp. Res.*, 2003, **35**, 271–278.
37 N. Michelutti, M. S. V. Douglas and J. P. Smol, *Global Planet. Change*, 2003, **38**, 257–271.
38 D. Antoniades, M. S. V. Douglas and J. P. Smol, *J. Paleolimnol.*, 2005, **33**, 349–360.
39 S. Payette, A. Delwaide, M. Caccianiga and M. Beauchemin, *Geophys. Res. Lett.*, 2004, **31**, L18208, DOI: 10.1029/2004GL020358.
40 I. Overeem, R. S. Anderson, C. W. Wobus, G. D. Clow, F. E. Urban and N. Matell, *Geophys. Res. Lett.*, 2011, **38**, L17503, DOI: 10.1029/2011GL048681.
41 C.-L. Ping, G. J. Michaelson, L. Guo, M. T. Jorgenson, M. Kanevskiy, Y. Shur, F. Dou and J. Liang, *J. Geophys. Res.*, 2011, **116**, G02004, DOI: 10.1029/2010JG001588.
42 W. D. Taylor, J. H. Carey, D. R. S. Lean and D. J. McQueen, *Can. J. Fish. Aquat. Sci.*, 1991, **48**, 1960–1966.

Open Access Article. Published on 18 October 2013. Downloaded on 9/6/2024 8:07:53 AM. This article is licensed under a Creative Commons Attribution 3.0 Unported Licence.

43 P. Larsson, L. Collvin, L. Okla and G. Meyer, *Environ. Sci. Technol.*, 1992, **26**, 346–352.
44 J. Dachs, S. J. Eisenreich and R. M. Hoff, *Environ. Sci. Technol.*, 2000, **34**, 1095–1102.
45 O. Berglund, P. Larsson, G. Ewald and L. Okla, *Environ. Pollut.*, 2001, **113**, 199–210.
46 L. Nizzetto, R. Gioia, J. Li, K. Borgå, F. Pomati, R. Bettinetti, J. Dachs and K. C. Jones, *Environ. Sci. Technol.*, 2012, **46**, 3204–3211.
47 S. G. Donaldson, J. Van Oostdam, C. Tikhonov, M. Feeley, B. Armstrong, P. Ayotte, O. Boucher, W. Bowers, L. Chan, F. Dallaire, R. Dallaire, E. Dewailly, J. Edwards, G. M. Egeland, J. Fontaine, C. Furgal, T. Leech, E. Loring, G. Muckle, T. Nancarrow, D. Pereg, P. Plusquellec, M. Potyrala, O. Receveur and R. G. Shearer, *Sci. Total Environ.*, 2010, **408**, 5165–5234.
48 R. J. Letcher, J. O. Bustnes, R. Dietz, B. M. Jenssen, E. H. Jørgensen, C. Sonne, J. Verreault, M. M. Vijayan and G. W. Gabrielsen, *Sci. Total Environ.*, 2010, **408**, 2995–3043.
49 F. Wania and D. Mackay, *Sci. Total Environ.*, 1995, **160/161**, 211–232.
50 Y. Su and F. Wania, *Environ. Sci. Technol.*, 2005, **39**, 7185–7193.
51 J. M. Armitage, S.-D. Choi, T. Meyer, T. N. Brown and F. Wania, *Environ. Sci. Technol.*, 2013, **47**, 923–931.
52 E. Carmack, D. Barber, J. Christensen, R. Macdonald, B. Rudels and E. Sakshaug, *Prog. Oceanogr.*, 2006, **71**, 145–181.
53 L. Sánchez-Garcia, V. Alling, S. Pugach, J. Vonk, B. van Dongen, C. Humborg, O. Dudarev, I. Semiletov and Ö. Gustafsson, Global Biogeochem. Cycles, 2011, **25**, GB2007, DOI: 10.1029/2010GB003862.
54 L. Coppola, M. Roy-Barman, P. Wassmann, S. Mulsow and C. Jeandel, *Mar. Chem.*, 2002, **80**, 11–26.
55 S. M. Trimble and M. Baskaran, *Mar. Chem.*, 2005, **96**, 1–19.
56 D. R. Griffith, A. P. McNichol, L. Xu, F. A. McLaughlin, R. W. Macdonald, K. A. Brown and T. I. Eglinton, *Biogeosciences*, 2012, **9**, 1217–1224.
57 S. B. Moran, K. M. Ellis and J. N. Smith, *Deep Sea Res., Part II*, 1997, **44**, 1593–1606.
58 K. Bahm and M. A. K. Khalil, *Chemosphere*, 2004, **54**, 143–166.
59 K. Breivik, A. Sweetman, J. M. Pacyna and K. C. Jones, *Sci. Total Environ.*, 2007, **377**, 296–307.
60 F. Wania, *Environ. Sci. Technol.*, 2003, **37**, 1344–1351.
61 J. Ma, H. Hung, C. Tian and R. Kallenborn, *Nat. Clim. Change*, 2011, **1**, 255–260.
62 S. Eckhardt, A. Stohl, S. Beirle, N. Spichtinger, P. James, C. Forster, C. Junker, T. Wagner, U. Platt and S. G. Hennings, *Atmos. Chem. Phys.*, 2003, **3**, 1769–1778.
63 Y. F. Lie, R. W. Macdonald, J. M. Ma, H. Hung and S. Venkatesh, *Sci. Total Environ.*, 2004, **324**, 115–139.
64 Ö. Gustafsson, P. Andersson, J. Axelman, T. D. Bucheli, P. Kömp, M. S. McLachlan, A. Sobek and J.-O. Thörngren, *Sci. Total Environ.*, 2005, **342**, 261–279.
65 K. Borgå, G. W. Gabrielsen and J. U. Skaare, *Mar. Ecol.: Prog. Ser.*, 2002, **235**, 157–169.
66 *The organic carbon cycle in the Arctic Ocean*, ed. Stein, R. and Macdonald, R. W., Springer-Verlag, Berlin, Germany, 2004.
67 M. B. Yunker, L. L. Belicka, H. R. Harvey and R. W. Macdonald, *Deep Sea Res., Part II*, 2005, **52**, 3478–3508.
68 R. Y. Dyda, M. T. Suzuki, M. U. Yoshinaga and H. R. Harvey, *Deep Sea Res., Part II*, 2009, **56**, 1249–1263.
69 J. E. Vonk, B. E. van Dongen and Ö. Gustafsson, *Geophys. Res. Lett.*, 2010, **37**, L11605, DOI: 10.1029/2010GL042909.
70 J. E. Vonk, L. Sanchez-Garcia, B. E. van Dongen, V. Alling, D. Kosmach, A. Charkin, I. P. Semiletov, O. V. Dudarev, N. Shakhova, P. Roos, T. I. Eglinton, A. Andersson and Ö. Gustafsson, *Nature*, 2012, **489**, 137–140.
71 F. A. P. C. Gobas and L. G. MacLean, *Environ. Sci. Technol.*, 2003, **37**, 735–741.

 This journal is © The Royal Society of Chemistry 2013